HHS Public Access

Author manuscript

J Vasc Interv Radiol. Author manuscript; available in PMC 2020 July 16.

Published in final edited form as:

J Vasc Interv Radiol. 2019 September ; 30(9): 1480–1486.e2. doi:10.1016/j.jvir.2019.03.004.

Transarterial Delivery of a Biodegradable Single-Agent Theranostic Nanoprobe for Liver Tumor Imaging and Combinatorial Phototherapy

Olena R. Taratula, PhD,
Department of Pharmaceutical Sciences, College of Pharmacy, Oregon State University, Portland, Oregon

Oleh Taratula, PhD,
Department of Pharmaceutical Sciences, College of Pharmacy, Oregon State University, Portland, Oregon

Xiangjun Han, MD,
Charles T. Dotter Department of Interventional Radiology, Oregon Health and Science University, 3181 SW Sam Jackson Park Road, L-605, Portland, OR 97239.

Younes Jahangiri, MD,
Charles T. Dotter Department of Interventional Radiology, Oregon Health and Science University, 3181 SW Sam Jackson Park Road, L-605, Portland, OR 97239.

Yuki Tomozawa, MD,
Charles T. Dotter Department of Interventional Radiology, Oregon Health and Science University, 3181 SW Sam Jackson Park Road, L-605, Portland, OR 97239.

Masahiro Horikawa, MD,
Charles T. Dotter Department of Interventional Radiology, Oregon Health and Science University, 3181 SW Sam Jackson Park Road, L-605, Portland, OR 97239.

Barry Uchida, RTR, BS,
Charles T. Dotter Department of Interventional Radiology, Oregon Health and Science University, 3181 SW Sam Jackson Park Road, L-605, Portland, OR 97239.

Hassan A. Albarqi, MS,
Department of Pharmaceutical Sciences, College of Pharmacy, Oregon State University, Portland, Oregon

Canan Schumann, PharmD, PhD,
Department of Pharmaceutical Sciences, College of Pharmacy, Oregon State University, Portland, Oregon

Shay Bracha, DVM, MS, DACVIM,
Carlson College of Veterinary Medicine, Oregon State University, Corvallis, Oregon

Tetiana Korzun, BA, BSc,

Address correspondence to K.F.; farsad@ohsu.edu.

Department of Pharmaceutical Sciences, College of Pharmacy, Oregon State University, Portland, Oregon

Khashayar Farsad, MD, PhD
Charles T. Dotter Department of Interventional Radiology, Oregon Health and Science University, 3181 SW Sam Jackson Park Road, L-605, Portland, OR 97239.

Abstract

Purpose: To assess the selective accumulation of biodegradable nanoparticles within hepatic tumors after trans-arterial delivery for in vivo localization and combinatorial phototherapy.

Materials and Methods: A VX2 hepatic tumor model was used in New Zealand white rabbits. Transarterial delivery of silicon naphthalocyanine biodegradable nanoparticles was performed using a microcatheter via the proper hepatic artery. Tumors were exposed via laparotomy and nanoparticles were observed by near-infrared (NIR) fluorescence imaging. For phototherapy, a handheld NIR laser (785 nm) at 0.6 W/cm^2 was used to expose tumor or background liver, and tissue temperatures were assessed with a fiber-optic temperature probe. Intra-tumoral reactive oxygen species (ROS) formation was assessed using a fluorophore H2DCFDA (2',7'-dichlorodihydrofluorescein diacetate).

Results: Nanoparticles selectively accumulated within viable tumor by NIR fluorescence. Necrotic portions of tumor did not accumulate nanoparticles, consistent with a vascular distribution. NIR-dependent heat generation was observed with nanoparticle-containing tumors, but not in background liver. No heat was generated in the absence of NIR laser light. ROS were formed in nanoparticle-containing tumors exposed to NIR laser light, but not in background liver treated with NIR laser or in tumors in the absence of NIR light.

Conclusions: Biodegradable nanoparticle delivery to liver tumors from a transarterial approach enabled selective in vivo tumor imaging and combinatorial phototherapy.

Introduction:

Transarterial liver-directed therapies for primary and metastatic liver cancer take advantage of the differential arterial blood supply to tumors (1). Although there has been progress in catheter-directed treatment options for primary and metastatic liver tumors, the procedure remains palliative with relatively modest improvements in median survival and time to disease progression (1-4). Despite the theoretical advantages of transarterial treatment, the lack of specificity, variability in treatment protocols, and the unpredictable response of the tumors to the available therapeutic challenges have limited the utility of this treatment regime. Transarterial embolotherapies are also potentially hepatotoxic , particularly in patients with poor liver function (5), and may additionally compromise hepatic blood flow (6, 7). Optimally, liver tumors would be treated with a highly targeted approach that safely and specifically destroys tumor cells while preserving functional liver parenchyma. Indeed, highly selective chemoembolization is recommended over less selective delivery to maximize the therapeutic profile and minimize toxicity (8). An ideal strategy would include high anatomic selectivity combined with tumor specificity.

Fluorescence imaging agents which are excitable in the near-infrared (NIR) spectrum reduce potential autofluorescence of background parenchyma, since most tissues have minimal light absorbance with NIR light (9). Real-time fluorescence imaging has shown promise for intra-operative visualization of tumors with growing interest as a targeting tool (10). NIR-excited agents can also be used for phototherapy. Combinatorial phototherapy can destroy cancer cells by generating both reactive oxygen species (ROS) with photodynamic therapy (PDT), and heat with photothermal therapy (PTT) under exposure to NIR light (11-16). Combining the capability for real-time imaging and phototherapy into a single agent, therefore, has high translational potential (17, 18). Indocyanine green (ICG) is an FDA-approved fluorescence imaging agent that has been used to identify hepatic tumors intra-operatively (19, 20). ICG, however, exhibits poor photostability, with the risk of photodegradation leading to loss of tumor detection during image-guided phototherapy (18).

Photostable silicon naphthalocyanine (SiNc) has recently been used to develop novel biodegradable photo-theranostic nanoprobes (SiNc-TN) (16, 17) capable of tumor-selective fluorescence imaging and phototherapy under NIR light (Fig 1). SiNc-TN selectively accumulate within tumors due to known enhanced permeability and retention (EPR) effects resulting in enhanced circulation time, tumor penetration and retention relative to unencapsulated small-molecule probes (21). Intravenous infusion of the nanoprobes at doses of 1.5-3.0 mg/kg, however, results in systemic absorption and requires up to twenty-four hours for adequate tumor uptake (16, 17). In this report, transarterial SiNc-TN delivery into liver tumors using a rabbit VX2 liver tumor model is examined for intra-operative tumor detection and combinatorial phototherapy.

MATERIALS AND METHODS

Preparation and Characterization

SiNc-TN used in this study was prepared via a solvent evaporation method according to a previously published protocol (16). Characterization of SiNc-TN properties is provided in Figure S1 with additional details. Cryogenic transmission electron microscopy (cryo-TEM) was used to characterize SiNc-TN morphology and size per prior protocol (16). Temperature change under NIR laser light (0.6 W/cm^2) was recorded during 20 minutes using a fiber-optic temperature probe. Fluorescence properties of SiNc-TN in solution were confirmed using an FDA-approved imaging system (Fluobeam® 800, Fluoptics, Cambridge, MA). Singlet oxygen ($^1O_2$) production by SiNc-TN was confirmed by singlet oxygen sensor green (SOSG) assay (See Supplementary Materials, SM).

Liver tumor implantation

Approval from the Institutional Animal Care and Use Committee was obtained for this pilot study. Nine New Zealand white rabbits (male and female, 2-3 kg, Charles River Laboratory, Cambridge MA) were used to develop a VX2 liver tumor model as previously described (22, 23). Two rabbits were used for hindlimb tumor propagation, and seven rabbits were used for liver tumor development using fresh or frozen harvested tumor fragments. Briefly, under general anesthesia, two 2 mm VX2 tumor fragments harvested from hindlimb tumors were implanted via a mini-laparotomy into the left lobe of the liver using a subxiphoid approach

with fine tip forceps and manual compression to achieve hemostasis. Two implantation sites were used to create two distinct tumors. The laparotomy was closed in layers, and the animals were recovered. In four rabbits, 1-2 mm tumor fragments were delivered percutaneously into the left hepatic lobe under ultrasound (US) guidance using a 14 gauge introducer needle. The hepatotomy was then sealed with small gelfoam pledgets. The animals were then monitored for tumor growth over a period of two to three weeks.

Transarterial Delivery of Nanoparticles to VX2 tumors

Ultrasound was performed to assess tumor growth to approximately 1-2 cm prior to the experiments. Rabbits were anesthetized and maintained with inhalational isoflurane gas. A small cutdown was performed to expose the femoral artery and a 4 French vascular sheath was inserted. A 4 French angled catheter (Glidecath, Terumo Medical, Somerset, NJ) was used to select the celiac artery, and a 1.7 French tapered microcatheter (Excelsior SL-10, Boston Scientific, Natick, MA) and a 0.010” microwire (Transend EX, Boston Scientific, Natick, MA) were coaxially advanced to selectively catheterize the proper hepatic artery. Angiography was performed to identify liver and tumor vasculature. Selective delivery of 0.3 mg/mL SiNc-TNs in saline prepared according to published protocol (16) was then performed over one minute with hand injection (1.5 mL total volume, 150-200 mcg/kg).

Real-time in vivo fluorescence monitoring and combinatorial phototherapy of tumors

To evaluate intratumoral ROS generation, a solution of a ROS sensitive fluorophore (2’,7’-dichlorodihydrofluorescein diacetate, H2DCFDA) was transarterially delivered into the tumors prior to exposure to NIR light. The ROS-activated agent was delivered transaterially 30 min prior to SiNc–mediated phototherapy to allow for tissue/cellular uptake. SiNc-nanoparticles were then delivered via selective transarterial delivery to the proper hepatic artery. After an additional 15 min, phototherapy was performed (785 nm laser at 0.6 W/cm^2).

After transarterial delivery of SiNc-TN, a laparotomy was performed to expose the liver and tumor implants under the Fluobeam® 800 NIR imaging device. Real-time fluorescence videos and images were recorded to evaluate SiNc-TN uptake and distribution. A 785 nm multi-mode fiber-coupled collimated laser (CW mode) system (Wavespectrum Laser, Inc., Beijing, China) was used to deliver NIR light energy for 2-5 minutes at 0.6 W/cm^2 for photoablation. One of the tumors in the left lobe was designated for targeted phototherapy and the other as an internal “dark” control to monitor baseline tumor necrosis and the effect of SiNc nanoparticles. Next, uninvolved background liver was also exposed to NIR light energy to serve as a “light” control to assess the baseline effect of laser energy on non-tumor tissue without accumulated nanoparticles. Thus, each animal served as their own treatment and internal control. During phototherapy, tissue temperature at the site of laser exposure and away from laser exposure was monitored every 10 seconds using a fiber-optic temperature probe implanted 2-5 mm into tumor or liver tissue surface. Following phototherapy, the animal was euthanized, and the following four tissue samples were collected for histological analysis: phototherapeutically treated tumor and liver tissues (tumor light and liver light) and untreated tumor and liver tissues (tumor dark and liver dark). Tissues, were embedded in paraffin and sectioned into 6-micron slices. After final

staining with the DNA staining fluorophore 4',6-diamidino-2-phenylindole (DAPI) to control for cell viability, the tissue samples were fluorescently imaged. Fluorescence images of each section were taken, and the ROS levels were assessed based on the fluorescence intensity as detailed below.

ROS detection

A solution of 2',7'-dichlorodihydrofluorescein diacetate (H2DCFDA) (Molecular Probes, Eugene, OR) in phosphate buffered saline (PBS, 1.6 mL, 100 μM) was transarterially delivered 30 mins prior to laser irradiation. After treatment, the tumors were removed and fixed in 10% PBS buffered formalin for 36 h before immunohistochemistry to analyze the tissue samples for the production of ROS. The tumor tissues were then fixed in formalin, embedded in paraffin, sectioned, and collected onto slides as previously reported (24). DAPI (4′,6-Diamidino-2-phenylindole dihydrochloride) was used to stain cell nuclei. Fluorescence imaging was performed with an EVOS FL Cell Imaging System (Life Technologies, Grand Island, NY) using two different channels: for DAPI ((Ex. 4340 nm, Em. 488 nm); for ROS (Ex. 490 nm, Em. 520 nm).

Results

Nanoparticles NIR imaging of hepatic tumors: real-time monitoring

Liver tumor implants were successfully established in six of seven rabbits, visibly identified with mini-laparotomy. The SiNc-TN (0.3 mg/mL, 150-200 mcg/kg, Fig. S2A) nanoprobes were delivered via the proper hepatic artery (Fig S2B). Immediately after transarterial SiNc-TN delivery, the nanoprobes accumulated within the tumors and were sufficiently fluorescent for visualization as compared to the surrounding liver tissue under real-time fluorescence imaging (Fig 2). *Ex vivo* NIR fluorescence imaging of the resected rabbit liver further confirmed the significantly higher nanoparticle accumulation via fluorescence in the tumors vs background liver (Fig 3).

Phototherapy assessment in vivo

ROS levels associated with photodynamic therapy were assessed based on the green fluorescence intensity generated by ROS-activated H2DCFDA (100 μM). Phototherapeutic effects in tumors compared to liver tissue without and with laser light treatment were compared (Fig 4). Tumor samples after phototherapy clearly showed a significant change in ROS generation as indicated by green fluorescence as compared to controls (Fig 4A) with ~ 5-fold increase ($P < 0.001$, Fig 4B).

Under NIR irradiation (Fig S2C), the intratumoral temperature increased from ~34 °C to 42 °C within 3 min, reaching a 43-44 °C plateau after 6 min (Fig 4C, red curve). In comparison, the temperature in non-tumoral liver tissue showed only ~ 2 °C change under the same 785 nm irradiation conditions, from ~ ~34 °C to 36 °C (Fig 4C, black curve). Temperature increase within the tumor after SiNc-TN accumulation was seen only in the presence of NIR light as shown by temperature graphs (Fig S3).

Discussion

Transarterial therapies for liver cancer theoretically can deliver high local concentrations of therapeutics while reducing non-tumoral parenchymal and systemic toxicity (8). Furthermore, for patients who are operative candidates, there remains an unmet need for sensitive and specific intra-operative tumor targeting (25). To date, a novel theranostic approach which offers the integration of both real-time diagnosis and in situ therapy has been limited by lack of optimal theranostic agents (26). To meet this need, the objective of this study was to develop and evaluate a phototheranostic nanoplatform that can be used for both tumor delineation with real-NIR imaging and targeted treatment with phototherapy. Non-toxic SiNc-loaded biodegradable nanoparticles (SiNc-TN) demonstrated NIR fluorescence after rapid intratumoral accumulation with transarterial delivery, a feature that makes them highly sensitive and specific for in vivo image-guidance. Using a rabbit orthotopic liver tumor model, selective SiNc-TN uptake by tumors enabled real-time NIR visualization and combinatorial phototherapy.

Combinatorial therapies, distinct from chemo- and radiotherapies, may complement liver tumor therapy. Phototherapy is an alternative that can effectively destroy cancer cells through heat production (PTT) and generation of reactive oxygen species (PDT) (11-15). Phototherapy has minimal side effects because it selectively kills cancer cells with nontoxic photoactive drugs, which are specifically activated by targeted light (27). Phototherapy can also be effective for treating multidrug-resistant cancer cells through therapeutic mechanisms distinct from chemo and radiotherapies (12, 13, 28). The fluorescence emitted by such photo-active drugs enables tracking of their accumulation within cancer tissue and allows for selective focusing of NIR light onto the tumors to activate phototherapeutic mechanisms (29, 30). SiNc-TN nanoprobes provide the distinct advantage of a single-agent capable of both fluorescence image-guidance and combinatorial phototherapy, and show promise as a nanotheranostic agent for liver tumors.

Delivery of the SiNc-TN nanoprobes via a transarterial route offers several benefits. With transarterial delivery, tumor uptake was achieved with an order of magnitude less dose compared to prior experience with IV administration (150 mcg/kg vs 1.5 mg/kg) (16, 17). As the biosafety profile of nanotherapeutics is a major source of concern by the FDA, this delivery technique offers major translational advantages. Furthermore, transarterial delivery would enable highly selective targeting via individual tumor-feeding arterial branches. Moreover, transarterial delivery resulted in rapid real-time accumulation in tumors compared with a twenty-four hour accumulation time with IV administration, a feature that would be beneficial for real-time operative or endoscopic image guidance (16).

This study has several limitations. 1) Notably, NIR light has limited tissue penetration (up to 1.5-2 cm) rendering NIR guidance best for imaging of exposed and relatively superficial tumors. The current iteration could be cumbersome for clinical translation as it would require transarterial access and operative exposure. Ideally, a transarterially delivered agent could also be used for specific drug delivery or an adjuvant minimally-invasive procedure. Options may include use of endoscopic or percutaneously inserted fiberoptic lasers (31, 32). Furthermore, photoacoustic imaging (PAI), which relies on NIR-stimulated ultrasonic

emission from tissues, can detect tumors at depths up to 4-6 cm with a resolution of <1 mm (33). A nanoplatform which incorporates PAI with potential drug delivery in a similar structure to SiNc-TN could have significant potential as a percutaneous nanotherapeutic agent. Future studies will be needed to investigate these potential applications for SiNc-TN. 2) In addition, as this was primarily a feasibility study, no overall tumor-specific or survival outcomes were performed. 3) Furthermore, heterogeneity of tumor uptake was noted with some uncertainty as to whether this was due to tumor necrosis, vascularity, or concentration of the delivered agent. 4) Moreover, quantification of tumor to background liver uptake, as well as systemic uptake with pharmacokinetic analysis was not performed and will additionally be important. Certainly, further work to expand the observations of this pilot study is warranted to optimize the nanoplatform to its best extent.

In summary, a single-agent SiNc-based biodegradable nanoplatform demonstrated selective tumor uptake via transarterial delivery in a rabbit VX2 liver cancer model. This agent was able to generate tumor-specific heat and reactive oxygen species after brief exposure to NIR light. Use of nanoprobes for combinatorial therapy of solid tumors in the liver is novel. Transarterial delivery shows promise for immediate and specific uptake of multifunctional nanoprobes for open resection, and future research may aim at expanding this platform for real-time percutaneous tumor detection and therapy.

Supplementary Material

Refer to Web version on PubMed Central for supplementary material.

ABBREVIATIONS

SiNc	2,3-naphthalocyaninato-bis(trihexylsiloxy)silane
PEG-PCL	methoxy poly(ethylene glycol)-b-poly(ε-caprolactone)
SiNc-TN	photo-theranostic nanoprobes
NIR	near-infrared
ROS	reactive oxygen species
H2DCFDA	2’,7’-dichlorodihydrofluorescein diacetate
DAPI	4’,6-diamidino-2-phenylindole
PBS	phosphate buffered saline
PDT	photodynamic therapy
PTT	photothermal therapy

References

[1]. Habib A, Desai K, Hickey R, Thornburg B, Lewandowski R, Salem R. Transarterial approaches to primary and secondary hepatic malignancies. Nat Rev Clin Oncol 2015; 12:481–9. [PubMed: 25985939]

[2]. Farsad K, Costentin CE, Zhu AX. Hepatocellular carcinoma with portal venous invasion: radiating new hope? JAMA Oncol 2018; 4:669–70. [PubMed: 29543953]

[3]. Kolbeck KJ, Farsad K. Catheter-based treatments for hepatic metastases from neuroendocrine tumors. AJR Am J Roentgenol 2014; 203:717–24. [PubMed: 25247935]

[4]. Wasan HS, Gibbs P, Sharma NK, et al. First-line selective internal radiotherapy plus chemotherapy versus chemotherapy alone in patients with liver metastases from colorectal cancer (FOXFIRE, SIRFLOX, and FOXFIRE-Global): a combined analysis of three multicentre, randomised, phase 3 trials. Lancet Oncol 2017; 18:1159–71. [PubMed: 28781171]

[5]. Raoul JL, Sangro B, Forner A, et al. Evolving strategies for the management of intermediate-stage hepatocellular carcinoma: available evidence and expert opinion on the use of transarterial chemoembolization. Cancer Treat Rev 2011; 37:212–20. [PubMed: 20724077]

[6]. Kohi MP, Fidelman N, Naeger DM, LaBerge JM, Gordon RL, Kerlan RK Jr. Hepatotoxicity after transarterial chemoembolization and transjugular intrahepatic portosystemic shunt: do two rights make a wrong? J Vasc Interv Radiol 2013; 24:68–73. [PubMed: 23176968]

[7]. Park BV, Gaba RC, Lokken RP. Liver infarction after drug-eluting embolic transarterial chemoembolization for hepatocellular carcinoma in the setting of a large portosystemic shunt. Semin Intervent Radiol 2016; 33:337–41. [PubMed: 27904254]

[8]. de Baere T, Arai Y, Lencioni R, et al. Treatment of liver tumors with lipiodol TACE: Technical Recommendations from Experts Opinion. Cardiovasc Intervent Radiol 2016; 39:334–43. [PubMed: 26390875]

[9]. Weissleder R A clearer vision for in vivo imaging. Nat Biotechnol 2001; 19:316–7. [PubMed: 11283581]

[10]. DSouza AV, Lin H, Henderson ER, Samkoe KS, Pogue BW. Review of fluorescence guided surgery systems: identification of key performance capabilities beyond indocyanine green imaging. J Biomed Opt 2016; 21:80901. [PubMed: 27533438]

[11]. Zilidis G, Aziz F, Telara S, Eljamel MS. Fluorescence image-guided surgery and repetitive Photodynamic Therapy in brain metastatic malignant melanoma. Photodiagnosis Photodyn Ther 2008; 5:264–6. [PubMed: 19356668]

[12]. Anbil S, Rizvi I, Celli JP, Alagic N, Pogue BW, Hasan T. Impact of treatment response metrics on photodynamic therapy planning and outcomes in a three-dimensional model of ovarian cancer. J Biomed Optics 2013; 18:098004.

[13]. Triesscheijn M, Baas P, Schellens JH, Stewart FA. Photodynamic therapy in oncology. Oncologist 2006; 11:1034–44. [PubMed: 17030646]

[14]. Molpus KL, Kato D, Hamblin MR, Lilge L, Bamberg M, Hasan T. Intraperitoneal photodynamic therapy of human epithelial ovarian carcinomatosis in a xenograft murine model. Cancer Res 1996; 56:1075–82. [PubMed: 8640764]

[15]. Kim JY, Choi WI, Kim M, Tae G. Tumor-targeting nanogel that can function independently for both photodynamic and photothermal therapy and its synergy from the procedure of PDT followed by PTT. J Control Release 2013; 171:113–21. [PubMed: 23860187]

[16]. Taratula O, Doddapaneni BS, Schumann C, et al. Naphthalocyanine-based biodegradable polymeric nanoparticles for image-guided combinatorial phototherapy. Chem Mater 2015; 27:6155–65.

[17]. Li X, Schumann C, Albarqi HA, et al. A tumor-activatable theranostic nanomedicine platform for nir fluorescence-guided surgery and combinatorial phototherapy. Theranostics 2018; 8:767–84. [PubMed: 29344305]

[18]. Li Y, Wen T, Zhao R, et al. Localized electric field of plasmonic nanoplatform enhanced photodynamic tumor therapy. ACS Nano 2014; 8:11529–42. [PubMed: 25375193]

[19]. Gotoh K, Yamada T, Ishikawa O, et al. A novel image-guided surgery of hepatocellular carcinoma by indocyanine green fluorescence imaging navigation. J Surg Oncol 2009; 100:75–9. [PubMed: 19301311]

[20]. Ishizawa T, Fukushima N, Shibahara J, et al. Real-time identification of liver cancers by using indocyanine green fluorescent imaging. Cancer 2009; 115:2491–504. [PubMed: 19326450]

[21]. Maeda H, Nakamura H, Fang J. The EPR effect for macromolecular drug delivery to solid tumors: Improvement of tumor uptake, lowering of systemic toxicity, and distinct tumor imaging in vivo. Adv Drug Deliv Rev 2013; 65:71–9. [PubMed: 23088862]

[22]. Lee KH, Liapi E, Buijs M, et al. Percutaneous US-guided implantation of VX-2 carcinoma into rabbit liver: a comparison with open surgical method. J Surg Res 2009; 155:94–9. [PubMed: 19181344]

[23]. White SB, Chen J, Gordon AC, et al. Percutaneous ultrasound guided implantation of VX2 for creation of a rabbit hepatic tumor model. PLoS One 2015; 10:e0123888. [PubMed: 25853660]

[24]. Taratula O, Schumann C, Duong T, Taylor KL, Taratula O. Dendrimer-encapsulated naphthalocyanine as a single agent-based theranostic nanoplatform for near-infrared fluorescence imaging and combinatorial anticancer phototherapy. Nanoscale 2015; 7:3888–902. [PubMed: 25422147]

[25]. Nguyen QT, Tsien RY. Fluorescence-guided surgery with live molecular navigation--a new cutting edge. Nat Rev Cancer 2013; 13:653–62. [PubMed: 23924645]

[26]. Jo SD, Ku SH, Won YY, Kim SH, Kwon IC. Targeted nanotheranostics for future personalized medicine: recent progress in cancer therapy. Theranostics 2016; 6:1362–77. [PubMed: 27375785]

[27]. Agostinis P, Berg K, Cengel KA, et al. Photodynamic therapy of cancer: an update. CA Cancer J Clin 2011; 61:250–81. [PubMed: 21617154]

[28]. Spring BQ, Abu-Yousif AO, Palanisami A, et al. Selective treatment and monitoring of disseminated cancer micrometastases in vivo using dual-function, activatable immunoconjugates. Proc Natl Acad Sci U S A 2014; 111:E933–42. [PubMed: 24572574]

[29]. Li Y, Lin TY, Luo Y, et al. A smart and versatile theranostic nanomedicine platform based on nanoporphyrin. Nature Commun 2014; 5:4712. [PubMed: 25158161]

[30]. Sheng Z, Hu D, Zheng M, et al. Smart human serum albumin-indocyanine green nanoparticles generated by programmed assembly for dual-modal imaging-guided cancer synergistic phototherapy. ACS Nano 2014; 8:12310–22. [PubMed: 25454579]

[31]. Bown SG, Rogowska AZ, Whitelaw DE, et al. Photodynamic therapy for cancer of the pancreas. Gut 2002; 50:549–57. [PubMed: 11889078]

[32]. Richter JA, Kahaleh M. Photodynamic therapy: Palliation and endoscopic technique in cholangiocarcinoma. World J Gastrointest Endosc 2010; 2:357–61. [PubMed: 21173912]

[33]. Beard P Biomedical photoacoustic imaging. Interface Focus 2011; 1:602–31. [PubMed: 22866233]

[34]. Taratula O, Patel M, Schumann C, Naleway MA, Pang AJ, He H. Phthalocyanine-loaded graphene nanoplatform for imaging-guided combinatorial phototherapy. Int J Nanomedicine 2015; 10:2347–62. [PubMed: 25848255]

[35]. Taratula O, Schumann C, Naleway MA, Pang AJ, Chon KJ, Taratula O. A multifunctional theranostic platform based on phthalocyanine-loaded dendrimer for image-guided drug delivery and photodynamic therapy. Mol Pharm 2013; 10:3946–58. [PubMed: 24020847]

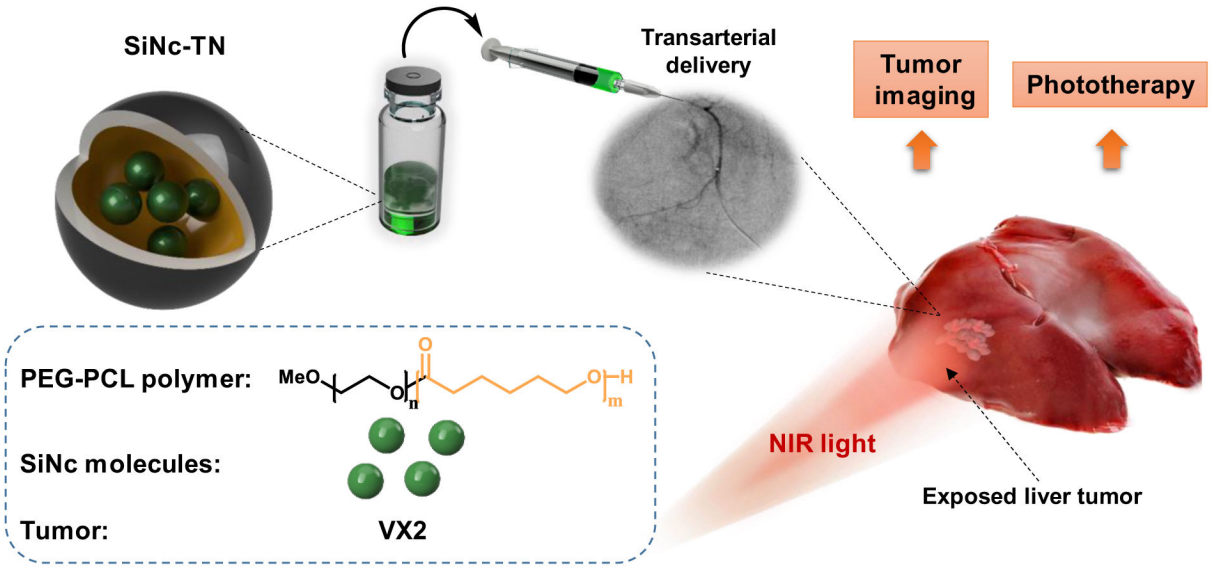

Figure 1.

Schematic illustration of a SiNc-based photo-theranostic nanoprobe (SiNc-TN) designed for tumor localization and subsequent combinatorial phototherapy. The nanoprobe consists of SiNc photoactive molecules encapsulated in the hydrophobic center of PEG–PCL polymeric nanoparticles. SiNc-TNs accumulate in tumors and can be detected via NIR fluorescence imaging. When irradiated with NIR laser light, SiNc-TNs transform the absorbed light energy into toxic ROS and heat to eradicate tumor tissue.

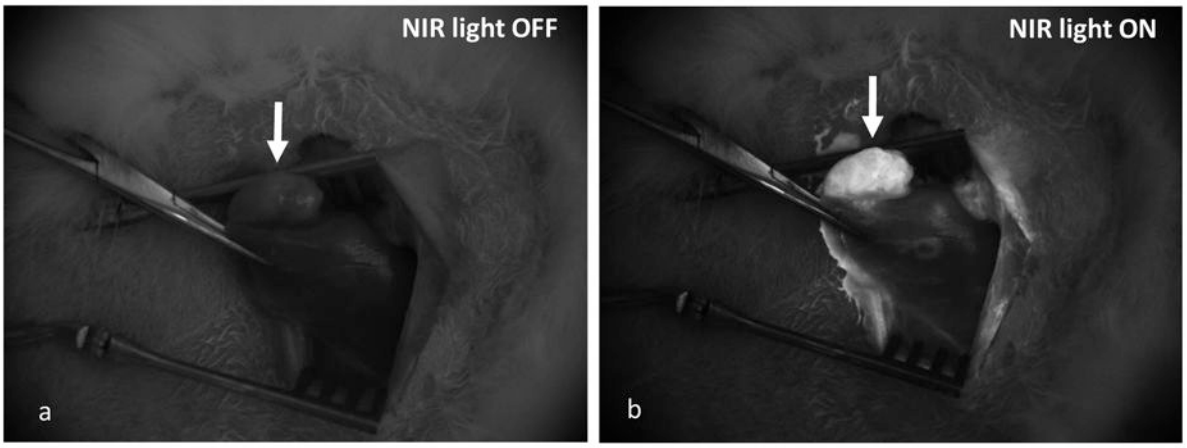

Figure 2.

Real-time in vivo NIR fluorescence images of VX2 carcinoma tumor after transarterial delivery of 150-200 mcg/kg SiNc-TN recorded with the Fluobeam®800 system: A, in the absence of NIR light; B, with NIR laser light ON.

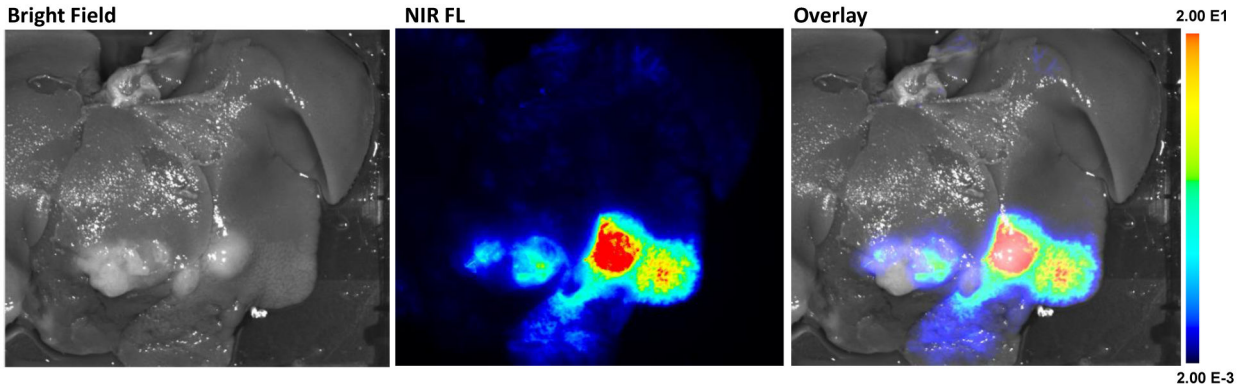

Figure 3.

NIR fluorescence images of VX2 carcinoma tumors in the liver collected by the Pearl Impulse Small Animal Imaging System 15 min after transarterial delivery of SiNc-TN.

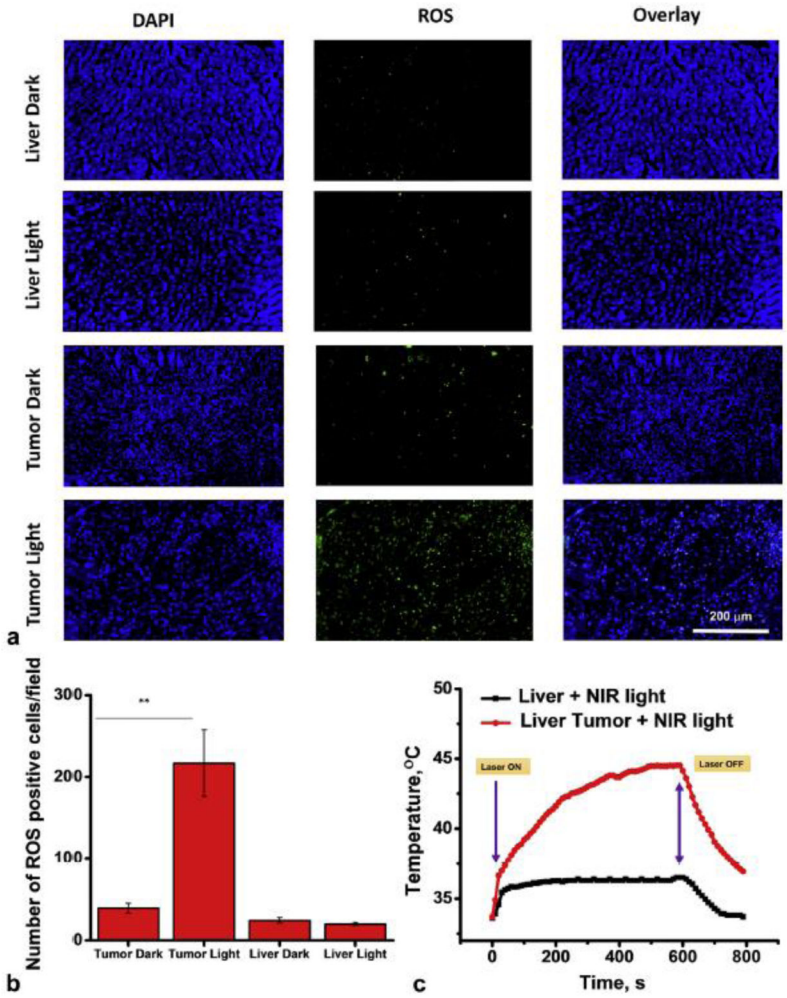

Figure 4.

Phototherapy of VX2 liver tumor implants using SiNc-TN: A, representative images of liver and tumor implant sections stained with DAPI (blue) for cell nuclei, and H_2DCFDA, a marker of ROS (green) where liver (control) and tumor tissues were harvested from the rabbit injected with SiNc-TN via transarterial delivery; B, mean numbers of ROS-positive cells per field of liver (control) and tumor sections; C, temperature profile inside of liver tumor implant recorded during the NIR phototherapy mediated by the SiNc-TN (red curve) with non-tumoral liver tissue exposed to NIR light used as the control (black curve) **P < 0.001 (n=3).